GEOCHRONOMETRIA 52 (2025) 208873
DOI 10.20858/geochr/208873

Available online at https://www.geochronometria.com/

THE HELIOS OSL READER: A PORTABLE SYSTEM FOR DATING AND DOSIMETRY APPLICATIONS

RENATA MAJGIER[1,2], KRZYSZTOF MATERNICKI[2], ARKADIUSZ MANDOWSKI[1,2], PIOTR MOSKA[3], MAGDALENA BIERNACKA[4,5] and SEBASTIAN KREUTZER[4]

[1]Institute of Physics, Faculty of Science and Technology, Jan Dlugosz University, Al. ArmiiKrajowej 13/15, 42-200, Czestochowa, Poland
[2]Zero-Rad Sp. z o.o., ul. Czartoryskiego 3/5, 42-200 Czestochowa, Poland
[3]Institute of Physics, Division of Geochronology and Environmental Isotopes, Silesian University of Technology, Konarskiego 22B str., 44-100, Gliwice, Poland
[4]Institute of Geography, Heidelberg University, Im Neuenheimer Feld 348, 69120 Heidelberg, Germany
[5]Institute of Physics, Faculty of Physics, Astronomy and Informatics, Nicolaus Copernicus University, Grudziadzka 5, 87-100 Toruń, Poland

Received 28 March 2025 Accepted 1 August 2025

Abstract
Optical Stimulated Luminescence (OSL) screening has emerged as a significant advancement in the field of luminescence dating applications. The employed portable luminescence readers offer practical and efficient tools for on-site measurements. In contrast to traditional luminescence dating in the laboratory, which often involves analyzing enriched quartz or feldspar mineral separates, portable OSL readers typically measure infrared (IR) or blue post-IR OSL signals from unprocessed bulk material. Here, we present a new device series that can be used as a portable OSL reader for dating purposes and luminescence screening: the OSL Helios reader. The reader has already been used in luminescence laboratories as a bench-top device for dosimetry research for almost twenty years. It recently received significant upgrades for better versatility. Our contribution demonstrates the application of the OSL Helios reader for luminescence screening on a loess profile, where luminescence signal intensities were assessed for specific sedimentological layers. The profile was measured using different versions of the OSL Helios reader, and the results were compared to those of the SUERC reader, which is commonly used as a portable reader in applications. Additionally, standard passive dosimeters (Al2O3:C and BeO), as well as detectors considered for emergency dosimetry (NaCl), were measured to determine the sensitivity of Helios devices. We conclude that the Helios reader performs similarly to the SUERC reader in most standard situations and can be considered an additional option for portable luminescence reader application.

Keywords
optically stimulated luminescence, portable OSL reader, luminescence dating, luminescence profiling

1. Introduction

According to the IPCC Sixth Assessment Report, further climate warming is expected to Optically stimulated luminescence (OSL, Huntley *et al.*, 1985) is a dosimetric technique that determines the time that has passed since a sample was last exposed to light or heat. It quantifies the release of energy in the form of light (luminescence) from dosimeters, such as natural minerals like quartz or feldspars. OSL measurements are typically performed with protocols that employ laboratory-based luminescence readers in a time- and resource-intensive procedure. As a result, many luminescence dating studies typically feature a relatively smaller number of ages, much less than would be desirable under ideal circumstances (Munyikwa *et al.*, 2021). An alternative and supplementing approach to dating utilizes portable luminescence readers, *e.g.*, which offer potential as an age profiling tool for sediments in a variety of depositional settings (Gray *et al.*, 2018). The

Corresponding author: R. Majgier
e-mail: renata.majgier@ujd.edu.pl

ISSN 1897-1695 (online), 1733-8387 (print)

portability of these devices enhances their usefulness, especially in field settings where preliminary analysis may be conducted immediately after sample collection. Consequently, in recent years, we have seen an increasing number of applications in dating and ionizing radiation dosimetry studies, as the following examples show. Portable OSL readers are used to measure luminescence signal intensities (*e.g.*, Gray *et al.*, 2019; Rizza *et al.*, 2024), which allows contextualization of the sediment stratigraphy (*e.g.*, Gray *et al.*, 2022) and interpretation of sediment processes dynamics to shed light on the depositional histories (Sanderson and Murphy, 2010; Muñoz-Salinas *et al.*, 2011). Additional examples of applications using portable luminescence readers include studies of coarse age assessments in various settings (*e.g.*, Srivastava *et al.*, 2023; Nitundil *et al.*, 2023; Turner *et al.*, 2021; Stone *et al.*, 2019, 2024; Porat *et al.*, 2019; Brill *et al.*, 2016; Ben-Melech *et al.*, 2024; Euzen *et al.*, 2024).

Most studies seem to employ variants of the SUERC portable OSL reader (Sanderson and Murphy, 2010). However, the first portable OSL reader was introduced by Poolton *et al.* (1994) for in field OSL measurements. Although other devices have been presented as well (*e.g.* Kook *et al.*, 2011), dating and screening application studies are limited. In a different dosimetric context, portable OSL readers are indeed interesting in case of radiological and nuclear emergency scenarios that require rapid action and on-site radiation dose assessment. Studies for this purpose were conducted with the SUERC (Karampiperi *et al.*, 2024), Helios (Mrozik *et al.*, 2017) or other, *e.g.* TL/OSL reader for on-site use in a large-scale radiological accident (Kim *et al.*, 2024). In medical dosimetry (like patient dosimetry, quality control of radiation therapy), portable OSL devices are already commonly used, mainly devices such as the microStar (Landauer Inc, Glenwood, USA), which is used with carbon-doped aluminium oxide detectors (Perks *et al.*, 2008) or myOSL (RadPro International GmbH, Remscheid, Germany) with a beryllium oxide detectors (Richter *et al.*, 2018). Other mobile readers were developed for, *e.g.*, thermoluminescence (Ikeya *et al.*, 1990) and electron-spin resonance (ESR) applications (Ikeya and Furusawa, 1989).

In general, portable readers offer several benefits, including easy transport to field sites, the ability to take measurements concurrently with sample collection, and simplicity in the measurement process. They can readily be applied outside the laboratory directly to bulk, unprocessed sediment, which significantly shortens the analytical process compared to traditional OSL dating. Samples are usually collected under a light-tight cover to prevent exposure to sunlight, typically by quickly inserting special opaque containers or tubes directly into the sediment or rock. Such samples are then either transported to the laboratory or placed directly into a portable reader and measured on-site under low-intensity amber or red light (*e.g.*, using a headlamp). Additionally, most common simple OSL devices allow for the analysis of larger sample quantities at a much faster rate and at a lower cost by using simple and quick protocols. However, the drawback for the portability is that those devices come without an ionizing radiation source and cannot perform routine dating protocols, such as the single aliquot regenerated (SAR, Murray and Wintle, 2000) dose protocol for OSL on quartz. Consequently, portable devices cannot readily be employed to generate chronometric ages in accordance with established protocols and are typically regarded as supplementary tools to conventional laboratory readers for preliminary analysis of sediments (Munyikwa *et al.*, 2021). Nevertheless, these devices have substantial potential, and further advancements in the development of portable luminescent devices are worth pursuing.

The aim of this work is to present the new portable OSL Helios reader for coarse dating applications and to compare its performance with the SUERC reader used in field measurements. The SUERC reader was selected for this comparison because it is widely used in the trapped-charge-dating community and hence defines our benchmark. The OSL Helios reader has already been successfully employed in dosimetry research (*e.g.* Marczewska *et al.*, 2016; Mrozik *et al.*, 2017; Marczewska *et al.*, 2019; Mrozik and Bilski, 2021). In this paper, we detail its usefulness in coarse screening procedures by measuring the luminescence response of a loess profile. Additionally, we report on the sensitivity of the device for standard dosimeters used in personal (Al_2O_3:C, BeO) and retrospective (NaCl) dosimetry.

2. Materials and methods

2.1. Measurement equipment

Two types of portable OSL readers were used in our study: (1) Helios (Zero-Rad, 2025, Mandowski *et al.*, 2010), in three variants, and (2) a SUERC portable OSL reader (Sanderson and Murphy, 2010); short: SUERC reader (see **Table 1** for an overview). A photo of the SUERC and Helios readers is shown in **Fig. 1a**. Additionally, a schematic diagram of the Helios reader is included in the supplement, **Fig. S1**.

The Helios reader family comprises several types of devices that can be adapted upon order for specific research or luminescent materials. The basic version of the reader (Helios-Basic) is equipped with one stimulation source and a sensitive detector operated in photon counting mode. It can perform basic OSL measurements, *e.g.* CW-OSL (continuous wave optically stimulated luminescence). The advanced version (Helios-Ex) facilitates one or two stimulation sources, extended detection also in the UV range (quartz windows) and various stimulation and detection modes. The measurements in this paper were performed using devices in the following versions: two Helios-Ex versions equipped with one stimulation source, green (Helios GR) and infrared (Helios IR), respectively, and one Helios-Ex version with two stimulation sources – blue and infrared (Helios BL/IR). The detailed stimulation

Table 1. *Overview equipment used for our experiments; further details see main text. A diagram of the stimulation and detection ranges of the devices is provided in Supplementary* ***Fig. S2****.*

TYPE	SUERC*	Helios family		
		Helios-Ex (Helios BL/IR)	Helios-Ex (Helios GR)	Helios-Ex (Helios IR)
Stimulation LED	470 nm - 880 nm	470 nm (± 20) nm - 850 (± 20) nm	- 525 (± 30 nm) -	- - 850 (± 20) nm
Stimulation filters	Schott GG420 (2 mm) / RG830 (2 mm)	Schott GG445 (2 × 3 mm) / RG715 (3 mm)	Schott GG495 (3 mm) + OG515 (3 mm)	Schott RG715 (3 mm)
Detection filters	Schott UG11 (12 mm)	Schott UG11-IRB (2 mm) + UG11 (3 mm) + UG1 (3 mm)	Schott UG11-IRB (2 mm) + UG11 (3 × 3 mm)	Schott BG39 (3 mm)
Detector	ETL PMT **	Hamamatsu H11870-02-Y005 with a quartz window	Hamamatsu H7360-02 with a quartz window	Hamamatsu H7360-02 with a quartz window

* *Information from Sanderson and Murphy (2010) and available upon delivery of the particular system in Heidelberg.*

** *SUERC PPSL 2 (Sanderson and Murphy, 2010) readers use photo detector modules incorporating selected 9124B tubes with 1" photocathodes and built in HV and amplifier-discriminator systems (Carter et al., 2018).*

and detection configuration for the different versions used is described below. Each Helios reader includes control electronics, a data interface, software for measurement control and data analysis, and an additional photosensor (Si photodiode S2386-5K, Hamamatsu, Japan) that controls the LED ring power density and ensures homogeneous illumination. The Helios reader is operated with the *Helios* software for Windows operating systems (see screenshot, **Fig. 1b**). Results are exported as ASCII files (*.osl) with a comma-separated value column structure. Data can be analysed in any standard software capable of importing comma-separated value files. Additionally, file import and analysis are supported in the R (R Core Team, 2025) package 'Luminescence' (Kreutzer *et al.*, 2024) through the functions `read_HeliosOSL2R()` and `analyse_portableOSL()`. Currently, Helios does not support exporting measurement data to the XLUM format (Kreutzer *et al.*, 2023) format. However, Helios .osl files can be converted easily to .xlum files using the R package 'xlum' (Kreutzer and Burow, 2022).

The green stimulation reader (Helios GR) consists of an illumination module containing 15 LEDs (peak wavelength at 525 nm, FWHM: 30 nm) with optical lenses and long pass filters, consisting of Schott filters GG495 and OG515, which are used to cut off the shortwave light component below 500 nm (**Table 1**). Luminescence detection is performed with an H7360-02 photomultiplier with a quartz window (Hamamatsu, Japan) through a Schott UG11-IRB and UG-11 filters (transmission: 240–400 nm). Samples are placed in aluminium holders with diameters ranging from 7 mm to 16 mm and a height of 4 mm (applies to all tested versions of the Helios reader).

The Helios-Ex reader with infrared stimulation (Helios IR) contains a ring with 15 LEDs (peak at 850 nm, FWHM 20 nm) and RG715 filters to block short-wave light components below 700 nm. Luminescence is detected using an H7360-02 photomultiplier with a quartz window (Hamamatsu, Japan) and equipped with a BG39 filter, covering the wavelength range of 300–600 nm.

The reader equipped with two types of stimulation sources (Helios BL/IR) uses six blue LEDs (peak at 470 nm, FWHM 20 nm) with cut-off filters GG455 and nine infrared LEDs (peak at 850 nm) with RG715 filters. Both OSL and IRSL are detected in the UV range (280–400 nm) using the H11870-02-Y005 photomultiplier (Hamamatsu, Japan) with a quartz window and optical filters: (1) a UV filter/NIR blocker (UQG Optics, England) based on Schott UG11-IRB with a dielectric coating and UG11 (transmission: 240–400 nm), and (2) an additional UG1 filter (transmission: 280–420 nm).

The SUERC reader provides pulsed and CW mode stimulation using infrared (880 nm) and blue (470 nm) LEDs. The system most widely distributed contains blue and IR LED diodes of 25 mW and 90 mW, respectively (Alghamdi *et al.*, 2024). The infrared stimulation light is filtered with a Schott RG830 and the blue LEDs with Schott GG435 filters. Luminescence is detected through UG11 filters by an ETL photodetector module with a 25 mm diameter bi-alkali photomultiplier, integral HV generator, amplifier–discriminator, and RS232–output photon counter (Sanderson and Murphy, 2010). Data analysis of the SUERC reader is likewise supported by the R package 'Luminescence' (Kreutzer *et al.*, 2024) and the functions `read_PSL2R()` and `analyse_portableOSL()`. The dimensions of the sample holder are as follows: lower diameter 50 mm, upper diameter 60 mm, height 19.5 mm. To measure the loess samples in our experiment, an additional 3D printed attachment was used in which a smaller aluminium holder from Helios was placed to ensure the same sample distribution in comparative measurements. A photo of the readers with sample holders is included in **Fig. S3**.

Fig. 1. *(a) Photo of SUERC (left) and Helios (right) readers for dimension comparison only; (b) Screenshot of Helios control software (v24.1). Helios's dimensions: length: 245 mm, width: 110 mm, height: 260 mm, weight: 4.8 kg.*

The stimulation intensity in the OSL Helios reader can be adjusted. The following current settings were used in our measurements: Helios BL/IR blue stimulation setting: 90 mA with a power density (irradiance at the sample position) of 1.5 $mWcm^{-2}$, infrared stimulation at 200 mA with a power density of 7.5 $mWcm^{-2}$; Helios GR green stimulation at 80 mA with an intensity of 1.2 $mWcm^{-2}$; and Helios IR infrared stimulation at 100 mA with an intensity of 2.0 $mWcm^{-2}$. The SUERC reader (Sanderson and Murphy, 2010) is operated with fixed values for the LED power of 25 mW and 90 mW for blue and infrared stimulation, respectively.

Measurements on all readers were performed in CW-OSL mode for 30 s for samples from the loess profile (Chap. 3.1) or 60 s (OSL detectors in Chap. 3.2) with sampling every second. For loess samples the OSL was first measured with infrared stimulation for 30s (IRSL), followed by 30 s blue-OSL or green-OSL as post-IR blue-OSL or post-IR green-OSL, respectively. It is assumed that 30 s of stimulation are sufficient for our experiments; however, in dating practices using a full protocol to determine an equivalent dose, significantly longer stimulation times are typically required to effectively erase the infrared (IR) signal from loess samples (Buylaert *et al.*, 2011). For the loess samples, the background, measured as the signal without the sample (30 s), was proportionally subtracted from IRSL or post-IRSL result. In the case of OSL detectors (Al_2O_3:C, BeO, NaCl), the background was determined as the detected light during 60 s of stimulation before any irradiation and subtracted from the measured signal after irradiation.

2.2. Loess samples

We selected a loess profile as a common application for portable readers in a geoscientific context. In contrast to sampling strategies with a high spatial resolution that would fully utilise the potential of portable luminescence readers, we used only stratigraphic positions already sampled for routine luminescence dating, which we deem sufficient for our comparison. The material investigated for our comparison was collected in 2023 from a newly prepared and documented loess profile at the Trzebnica brickyards site (**Fig. 2**) (51°18'44" N, 17°4'14" E, 193 m a.s.l.). The site has been known since the early 20th century and is today located in the northeastern part of Trzebnica (Poland) (Winnicki, 1997). The area is part of the Trzebnica Hills, which extend in a latitudinal range of approximately 50 km in length and 5–10 km in width.

The basic lithology of the studied profile can be presented as follows: the uppermost 50 cm consists of an A horizon of brown soil, followed by horizon B extending to approximately 110 cm, characterized by numerous vertical root channels with dark colouration followed by four meters of laminated loess. Between 5.4 m and 6 m, we observed transformed loess with an accumulation of carbonate concretions. From 6 m to 7.6 m, laminated loess continues, while at the base of the profile, a deflation pavement and a clay layer are present. Samples were collected using thin-walled steel pipes from Eijkelkamp system for sampling (Moska *et al.*, 2021). The collected loess samples were stored in the dark until measurement. Samples each weighing approximately 30 ± 3 mg were placed into the holder of the SUERC or Helios reader under a low red ambient light using a measuring cup. The samples were neither chemically nor physically processed except for gentle crushing to destroy aggregates and to achieve an even distribution. For each sampling position, the luminescence signals were always measured on three sub-samples, and

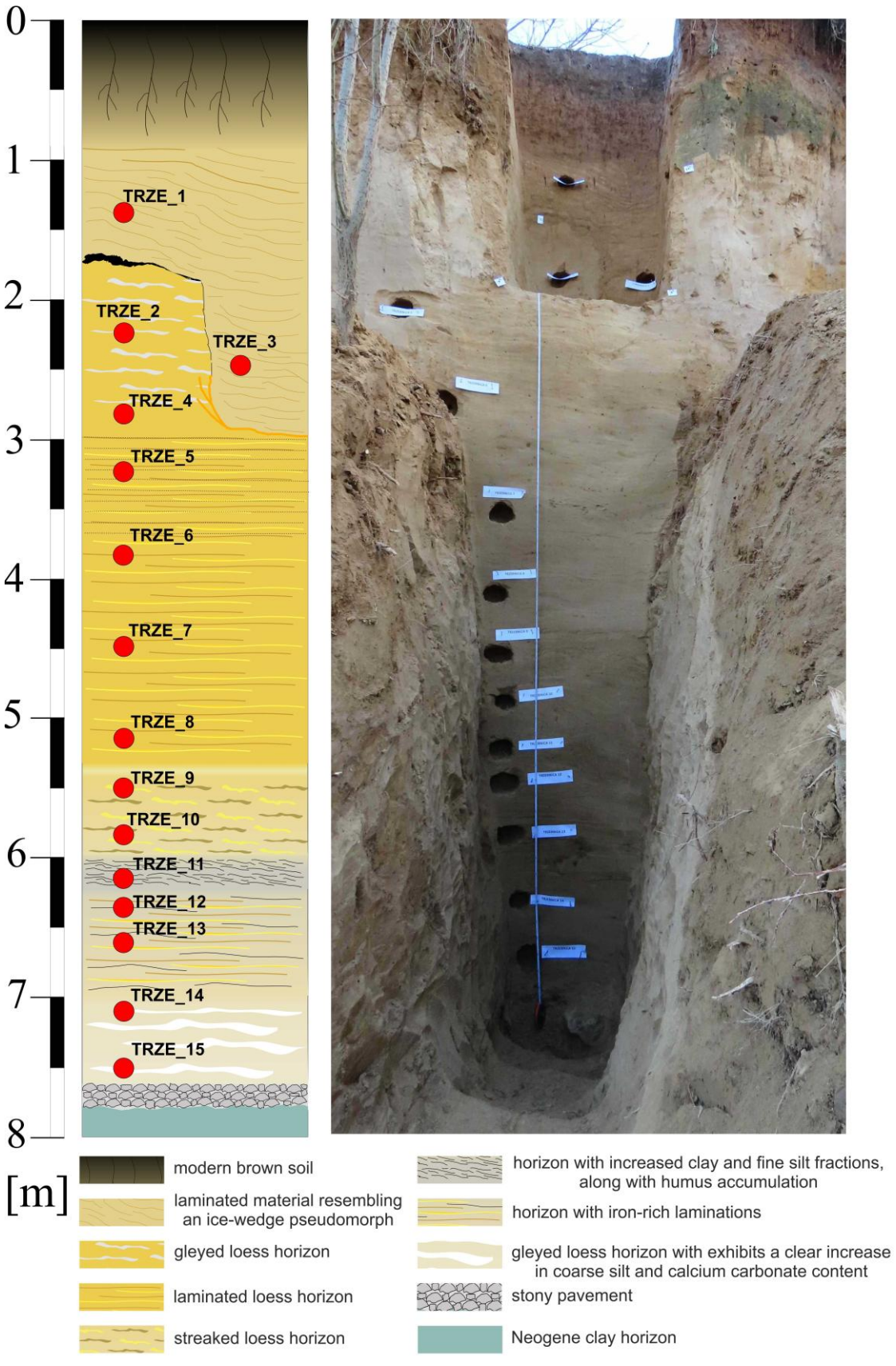

Fig. 2. *Profile sketch and photo of the loess profile at Trzebnica brickyards with the sample collection points and basic lithology.*

the resulting signal is the average of these three measurements. Measurement uncertainties shown in the figures were determined as the standard deviation of the mean.

2.3. OSL dosimeters

The intensity of the OSL signal, and thus the detection limit of the reader-detector system, depends on the stimulations used, the detection range, and the spectral properties of the detectors. To assess the sensitivity of the readers, passive dosimeters typically used in OSL dosimetry (for a primer, see Yukihara *et al.*, 2022) were employed: Al_2O_3:C (Landauer Inc., USA) with a diameter of 5 mm and a thickness of 1 mm and BeO (Thermalox995, Materion, USA) with dimensions 5×5×0.5 mm, as well as table salt pellets similar to those considered as detectors in retrospective and emergency dosimetry (Alghamdi *et al.*, 2022; Karampiperi *et al.*, 2024). For Al_2O_3:C ultraviolet emissions at 335 nm and 420 nm are reported (Yukihara and McKeever, 2006), as well as a dominant OSL emission band at ~415 nm (Denis *et al.*, 2011). The OSL emission spectrum of BeO for stimulation with 550 nm light ranges from 250 nm to 450 nm with two OSL emission bands at ~310 nm and ~370 nm (Yukihara, 2011). For NaCl, we could not identify OSL emission studies, beyond reference to several TL emission peaks, notably at ~590 nm and ~370 nm, additionally blue-OSL (stimulation: 470 nm; detection: UV-range) with higher sensitivity than IRSL (880 nm stim./orange det.) (Spooner *et al.*, 2011) and confirmation of OSL signal response.

Measurements using Al_2O_3:C and BeO were performed on single samples, which were each thermally reset by annealing at 500°C for 2 min, which was experimentally determined as sufficient to entirely deplete the detector signal, by placing them in the heated oven (FCF 2,5SHM, Czylok, Poland) and quickly removing after the set time. The temperature and duration of thermal resetting were determined experimentally and assumed sufficient for the measurements presented. NaCl chips of 4 mm diameter, 0.6 mm thickness and weight of 17 ± 1 mg were obtained by hard pressing table salt (FalksaltfintBergsalt, Sweden) with grain sizes of 250–400 µm under a pressure of 2 t. A series of NaCl chips were used for the measurements, *i.e.*, each measurement was made using a new NaCl sample. The detectors were irradiated with a $^{90}Sr/^{90}Y$ beta source, delivering a manufacturer specified dose rate of $7.6 \cdot 10^{-4}$ Gy s^{-1}.

For each administered dose, a given detector was measured once immediately after irradiation (fixed time of one minute measured with a stopwatch). For OSL measurements using the SUERC reader, samples were placed each time on the same marked location in the holder and the drawer was closed carefully to avoid movements to ensure the best possible repeatability. In the Helios reader, a 6 mm diameter holder guaranteed a repeatable sample position every time.

The minimum detectable dose (MDD) was calculated as the ratio of the background signal level (three standard deviations of the background signal) to the luminescence signal per unit radiation dose following commonly used procedure (*e.g.*, Bernhardsson *et al.*, 2009, Rawat *et al.*, 2014). The signals from unirradiated samples were used as background, *i.e.* OSL readout of 60 s was performed on a sample that was not previously irradiated (or was zeroed). The mean background value and standard deviation were determined from ten measurements. The background was determined separately for each reader-detector configuration. Additional measurements were also performed without any sample in the holder. These tests confirmed that the background level was the same both with the unirradiated sample and without any sample. The linear fitting parameters were used to determine the sample sensitivity (mGy^{-1}) required to find the detection limit according to the following procedure. The signal-to-dose coefficient was determined as the slope of the line fitted to the dose-response curve over the entire range of tested doses, along with its uncertainty obtained from the fitting parameters.

All experimental parameters, including irradiation conditions, waiting time, sample transfer under red light, and the method of OSL signal readout, were consistently maintained throughout the study to ensure the highest possible reproducibility of the results. However, it is important to acknowledge that the waiting period between irradiation and measurement was limited to approximately one minute and timed using a stopwatch. Although this approach allowed for controlled timing, measuring the luminescence signal shortly after irradiation may result in greater observed signal instability, as compared to measurements performed after a longer post-irradiation storage period that allows transient components to decay and the signal to stabilize.

3. Results

3.1. Luminescence profile of loess samples

The measurement results of samples from the loess profile illustrate the dependence of the OSL signal on profile depth (**Fig. 3**). The data in **Fig. 3** were normalized to the range from minimum (0) to maximum (1) to better illustrate the *signal pattern*. The absolute count values are shown in Supplementary **Fig. S4**. **Fig. 3a** shows a comparison of IRSL signals for the three readers used. **Fig. 3b** shows the post-IR blue-OSL results obtained with the SUERC and Helios BL/IR reader, and **Fig. 3c** additionally shows the post-IR signal measured for green-OSL with the Helios GR reader. For all presented signals, the overall *signal pattern* for the profile is similar for all readers, although the pattern obtained with SUERC is more pronounced, showing clearer peaks and stronger contrast. This likely related to the pulsed-stimulation of the SUREC with its background subtraction in the dead-times.

For infrared stimulation, the order of magnitude for photon counts (**Fig. S4a**) is similar for all readers (10^4–10^5 counts). For post-IR blue-OSL, photon counts are of the order of 10^5 counts for both Helios readers, with the SUERC reader producing giving a significantly higher signal,

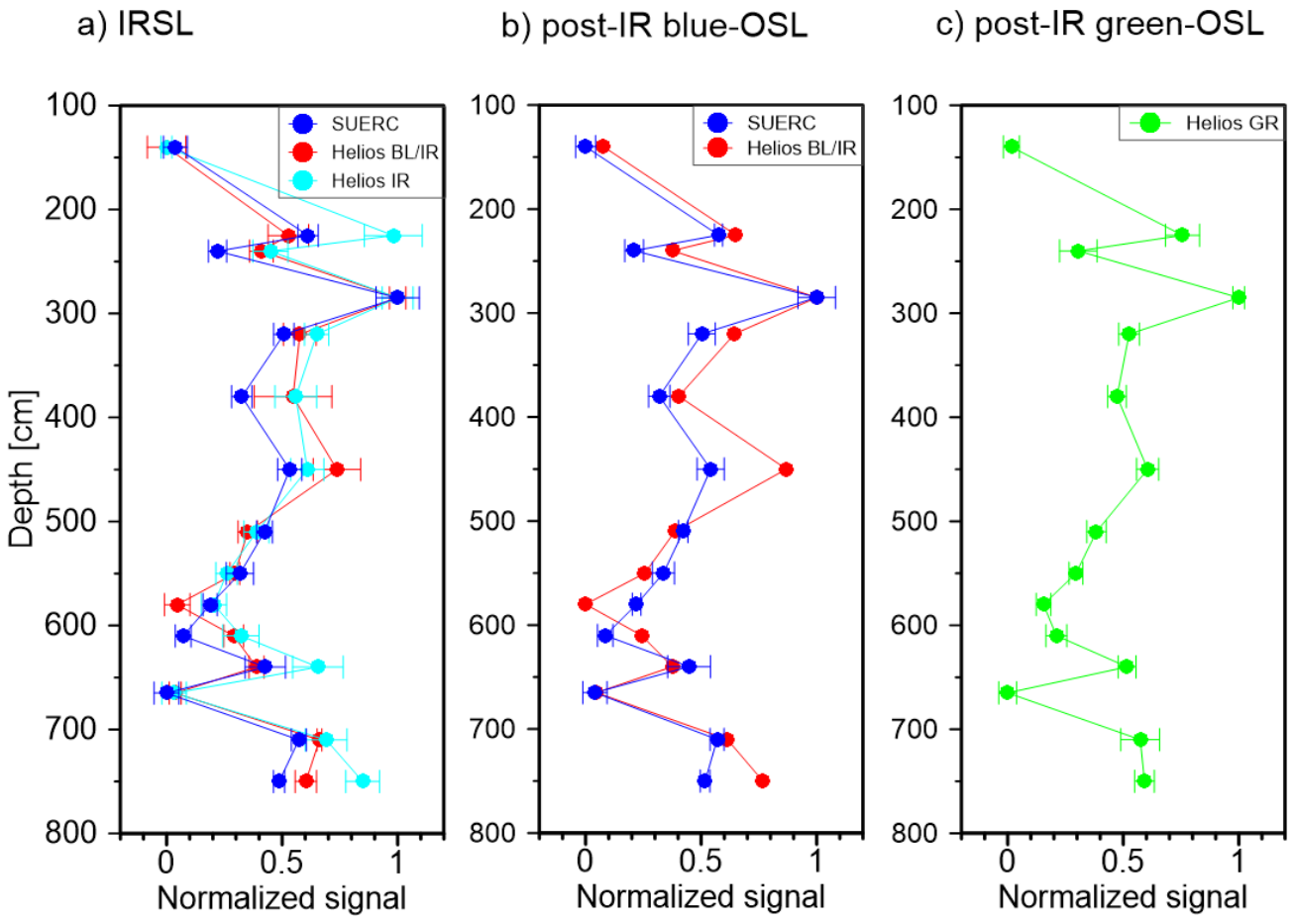

Fig. 3. *Luminescence profile measured using SUERC and Helios readers: a) IRSL, b) post-IR blue-OSL, c) post-IR green-OSL. Luminescence intensities (normalized to the range from minimum zero to maximum one) versus profile depth are shown and refer to the measurement parameters described in the text.*

approximately twice as large. While **Fig. 3b** shows the general profile pattern, a direct comparison of the blue-OSL signals for Helios BL/IR and SUERC can be found in **Fig. S4b**. Fewer counts than for post-IR blue-OSL were obtained for post-IR green-OSL in the Helios GR reader (**Fig. S4c**), of the order of 10^4 counts, which can be attributed to the generally lower bleaching efficiency of green light compared to blue (for quartz, *e.g.* Bøtter-Jensen *et al.*, 1999; Singarayer and Bailey, 2003; Chruścińska and Przegiętka, 2005).

The repeatability of the measurement can be characterized by the relative standard deviation (c_v), which was determined for three natural sub-samples each (at each sampling position, luminescence was measured on three subsamples). For the SUERC reader, the total number of averaged results are 30 (15 with blue stimulation and 15 with infrared stimulation), while for the Helios readers, it is 60 (15 with blue, 15 with green, and 30 with infrared stimulation). For all measurements, the relative standard deviation was always less than 25%. For the Helios readers, 42 out of 60 results (70%) had a c_v of less than 10%, while for the SUERC reader, 13 out of 30 (43%) had a c_v of less than 10%. The values of the relative standard deviations are given in **Table S1**.

3.2. Reader sensitivity

Because the setup of the readers differs slightly, we compared the detection sensitivities of the Helios and the SUERC reader using standard passive dosimeters after irradiation with doses of different orders of magnitude: 10 mGy, 100 mGy and 1000 mGy. The obtained dose responses for Al_2O_3:C, BeO, and NaCl for blue and green stimulation are shown in **Fig. 4**, while the IRSL response is shown for NaCl only in **Fig. 5**.

The order of magnitude of the total signal from the blue stimulation is similar for SUERC and Helios BL/IR readers (**Fig. 4**). A higher signal was obtained using the SUERC reader for Al_2O_3:C and BeO, while for NaCl, the signal was the highest with the Helios BL/IR reader. This difference is likely due to the combined effects of the emission characteristics of each material and the optical detection components of the specific readers. In Helios readers,

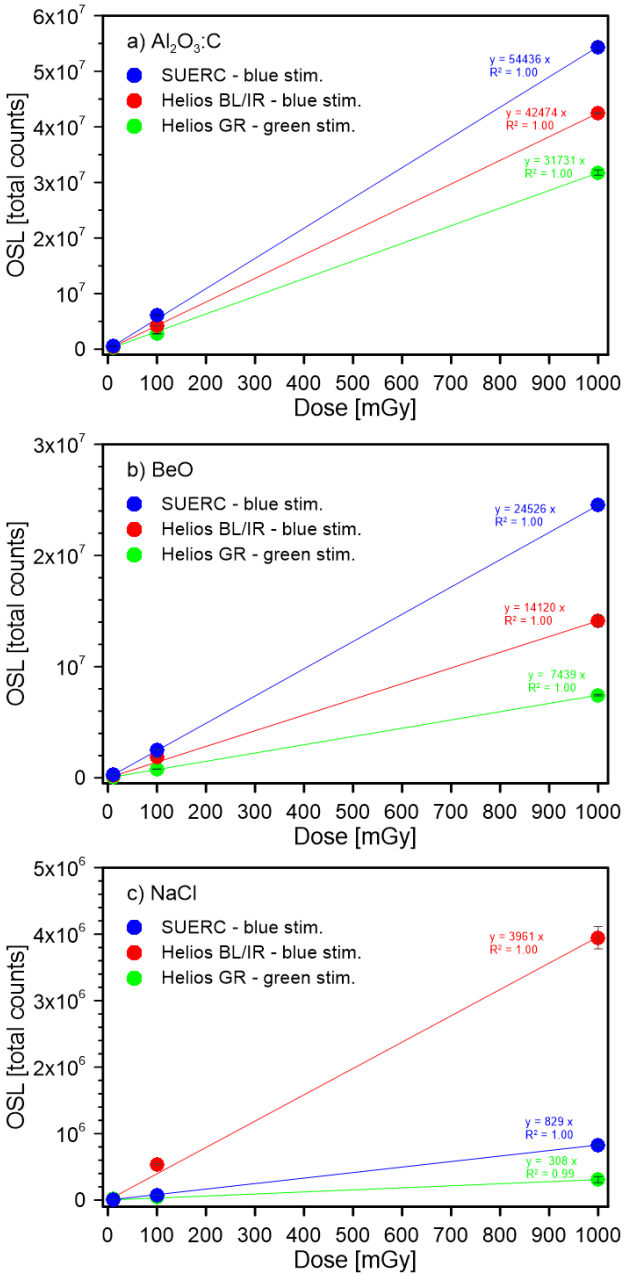

Fig. 4. *Dose dependency of the total OSL signal for a) Al_2O_3:C, b) BeO, and c) NaCl under blue (SUERC, Helios BL/IB) and green (Helios GR) stimulation. The continuous line indicates a fit of a straight-line function through the origin to the measurement points.*

the signal from green stimulation was lower than that from blue stimulation for all samples.

For infrared stimulation (**Fig. 5**), the highest number of counts was obtained using the Helios IR reader, and the lowest was for SUERC. Helios BL/IR and SUERC showed a similar order of magnitude of the signal, with Helios BL/IR providing more counts. This is due to the fact that the detection range of SUERC and Helios BL/IR is similar (about 280–400 nm), while for Helios IR, it is much wider

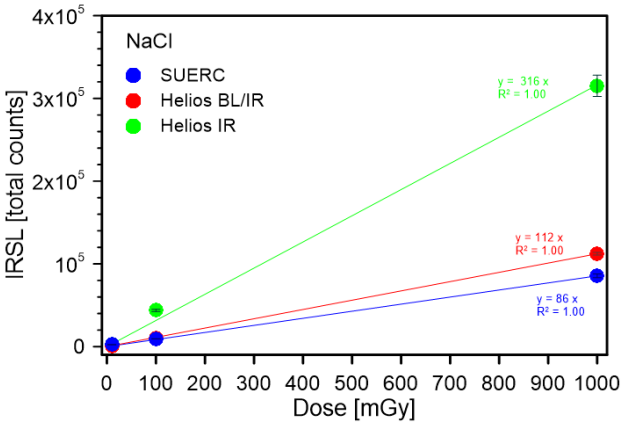

Fig. 5. *Dose dependency of the total IRSL signal for NaCl measured with SUERC, Helios BL/IB and Helios IR. The solid line indicates a fit of a straight line through the origin to the measurement points.*

(300–600 nm) and thus covers more emissions from the OSL detectors. The high signal with infrared stimulation was obtained for NaCl, which is related to the spectroscopic properties of the material and the range of stimulation to which the material is sensitive (Spooner *et al.*, 2011, Rodriguez-Lazcano *et al.*, 2012, Hunter *et al.*, 2012). In the case of Al_2O_3:C and BeO, infrared stimulation is not effective, which is in accordance with the characteristics of the dosimeters (Bulur *et al.*, 1998, Umisedo *et al.*, 2010, Yukihara *et al.*, 2016). Therefore, the IRSL results for these materials are not shown in this study.

For all tested detector types, a linear response was observed within the dose range of 10–1000 mGy under blue and green stimulation (**Fig. 4**). In the case of infrared stimulation, linearity was confirmed only for NaCl (**Fig. 5**). A straight line with a high R^2 value was fitted to the measurement points, representing the average counts per dose in the tested range and serving as a basis for determining the minimum detectable dose (MDD). **Figs. 4** and **5** include linear fits for all tested detectors under blue and green stimulation, as well as for NaCl under infrared stimulation.

Since only one measurement was performed for each detector at each dose level, individual measurement uncertainties (of significance) were not directly available. Therefore, an indirect method was used to estimate uncertainties based on the residuals from a linear fit through the origin, assuming a proportional relationship between the uncertainty and dose. The calculated uncertainties for each detector type are shown in **Figs. 4** and **5**. For the Al_2O_3:C and BeO detectors, uncertainties do not exceed 5%. Similarly, most NaCl measurements also exhibit uncertainties below 5%, except for 3 out of 18 measurements with the Helios readers, where higher uncertainties were observed.

3.3. Quantifying the minimum detectable dose (MDD)

The obtained MDD values are presented in **Table 2**. The orders of magnitude of MDD are similar for the SUERC

Table 2. *Minimum detectable dose (MDD) values were determined for the tested readers using Al_2O_3:C, BeO and NaCl detectors.*

READER	STIMULATION	MDD per DOSIMETER (µGy)		
		Al_2O_3:C	BeO	NaCl
SUERC	blue	21.2 ± 0.2	47.1 ± 0.1	1390 ± 10
Helios BL/IR	blue	88.2 ± 0.1	265.0 ± 5.0	950 ± 20
Helios GR	green	20.4 ± 0.2	87.1 ± 0.3	2100 ± 110
SUERC	infrared			560 ± 10
Helios BL/IR	infrared			560 ± 10
Helios IR	infrared			510 ± 10
Literature data	blue	4-57 [*1]	10 [*4]	2-47[*5,6](14600[*5])
Literature data	green	10 [*2]	nd.	nd.
Literature data	infrared	100 [*3]	nd.	340 [*6]

*[*1] Rawat et al. (2014), [*2] Kreutzer et al. (2018), [*3] Bulur et al. (1998), [*4] Yukihara et al. (2016), [*5] Karampiperi et al. (2024), [*6] Alghamdi et al. (2022)*

reader and the Helios readers. For Al_2O_3:C, blue/green stimulation yielded a MDD of several tens of µGy (~10^{-5} Gy), for BeO, several tenths or hundredths of µGy (~10^{-5} Gy – 10^{-4} Gy), and for NaCl, about 1–2 mGy (~10^{-3} Gy). In the case of infrared stimulation of NaCl, all readers yielded comparable results, with MDD around 0.5 mGy.

4. Discussion

In the study of loess profiles, the lower number of counts with blue stimulation in the Helios BL/IR reader compared to the SUERC reader likely is related to differences in the reader settings, such as the intensity of the stimulating light and slightly different detection efficiencies (filter configuration). It should be noted that the blue stimulation power in the tested Helios BL/IR reader is relatively low (~1.5 mWcm^{-2}) and probably lower than in SUERC (the power density for the SUERC reader is not specified). However, the Helios reader settings can be optimized at the production stage for a given application by adjusting the number and type of LEDs (and thus the stimulation intensity), as well as the detection range (PMT and optical filters).

In Helios readers, green stimulation typically yields fewer counts than blue due to its generally lower bleaching efficiency, as also observed in our measurements of loess samples composed of feldspar and quartz. The IRSL measurements are dominated by a feldspar signal, while the post-IR blue-OSL targets the remaining quartz signal (Thomsen *et al.*, 2008). Although the green stimulated quartz signal measured in the UV has a lower photo ionisation cross-section (Singarayer and Bailey, 2003) and is hence less efficient at stimulating quartz, it is still possible to obtain a high signal with a consistent profile (*i.e.* the luminescence signal maintains a stable and reproducible pattern under consistent experimental conditions).

The OSL emission spectrum of quartz and feldspars – the main components of loess samples – consists of several characteristic bands. For quartz, the dominant emission occurs at wavelengths of about 365 nm or 380 nm (*e.g.*, Huntley *et al.*, 1991, Lomax *et al.*, 2015), while for feldspars these are bands in the range of 280–290 nm, 320–340 nm, 390–440 nm and 550–570 nm, with most sedimentary feldspars showing dominant emission in the range of 400–410 nm (*e.g.*, Baril and Huntley, 2003, Lomax *et al.*, 2015). This emission largely overlaps with the detection window used in the SUERC and Helios BL/IR systems (approx. 280–400 nm), and with the wider detection range of the Helios IR system (300–600 nm). Despite the wider detection range of Helios IR, no higher signal is observed for infrared stimulation compared to other readers, which is due to the lack of material emission in the range corresponding to the maximum sensitivity of the photodetector in Helios IR (*i.e.* above 400–500 nm).

The results for relative standard deviation of samples from loess profiles show that the measurement repeatability for both readers is comparable and considered sufficient, given the application. The obtained values of standard deviation are typical for measurements of natural samples (*e.g.* Thomsen *et al.*, 2005, Guérin *et al.*, 2015, Kinnaird *et al.*, 2015), reflecting both experimental uncertainty and inherent variability related to material composition, geological origin, and grain heterogeneities.

The sensitivity of SUERC and Helios readers for standard OSL dosemeters was investigated, and the obtained values of MDD can be roughly compared with literature data. These data report a minimum detection limit of 10 µGy for Al_2O_3:C (Kreutzer *et al.*, 2018) using the lexsyg SMART reader (Richter *et al.*, 2015) with green stimulation at measurement temperature of 70°C and the detection centred at 410 nm. Other MDD values ranging from 4 µGy to 57 µGy were obtained for Al_2O_3:C under blue stimulation depending on the stimulation intensity and signal integration time (Rawat *et al.*, 2014). Additionally, doses as low as 100 µGy have been detected for Al_2O_3:C with infrared stimulation using the Risø TLDA 10 (DTU National Laboratory) reader (Bulur *et al.*, 1998). The magnitude of the obtained results is comparable to those presented here for Al_2O_3:C, which we consider satisfactory in the absence of a dedicated study that would replicate all instrumental settings as closely as feasible.

For BeO, literature data report an MDD of 10 μGy for blue stimulation (Yukihara *et al.*, 2016), while we obtained consistently larger values for all used equipment ranging from ca 47 μGy (SUERC) to 265 μGy (Helios BL/IR) for blue stimulation. The reasons are unknown and would require a dedicated study, which is beyond the scope of this manuscript.

Measurements of NaCl chips using the SUERC reader gave MDD in the range of 2–47 μGy (Karampiperi *et al.*, 2024); however, it should be noted that readouts were taken for five chips simultaneously because, for less than five chips, the signal was very low and not properly distinguishable for the low dose (14.6 mGy). Likewise, Alghamdi *et al.* (2022) obtained MDD values on NaCl of 7 μGy for blue stimulation and 340 μGy for IRSL for a comparable system but for a sachet of 1 g of NaCl. On the contrary, our measurements using SUERC and Helios readers were performed on one identical chip and gave a sensitivity of about 1 mGy for blue stimulation and 0.5 mGy for infrared stimulation. The resulting sensitivity of the Helios reader should be sufficient for dosimetry and dating applications.

5. Conclusions

We have shown that the portable OSL Helios reader can be used for luminescence profile screening, similar to other devices of this type, such as the SUERC reader, which we used for a benchmark comparison here.

For a more particular application that is relevant to archaeology and geoscience, we sampled a loess profile and measured the corresponding signal from infrared stimulation followed by blue or green stimulation (post-IR blue-OSL and post-IR green-OSL, respectively). The pattern of the signal response through the profile obtained with the Helios reader are like those of the SUERC reader typically used for this type of application, although absolute intensities sometimes vary. The measurement repeatability of the Helios reader has a relative standard deviation (c_v) of <=25% for measurements using three samples of natural material. Additionally, most of the measurement points in loess profiles measured using Helios (70%) have a c_v of less than 10%. Similar repeatability is observed for the SUERC reader, with a maximum c_v of 23% and the majority of points (60%) having c_v above 10%.

The Helios reader can also be used to measure passive detectors for ionizing radiation dosimetry. Based on the MDD results for standard OSL detectors, we conclude that the sensitivity of the Helios reader is high (*e.g.*, for Al_2O_3:C with blue light stimulation, the MDD is 0.09 mGy) and comparable to other portable OSL devices such as the SUERC reader (0.02 mGy for Al_2O_3:C with blue stimulation).

The advantage of the Helios family readers is the wide selection of stimulation sources, adjustable stimulation intensity, and a compact/modular design that allows for easy device operation in non-laboratory conditions. The modular design of the family of Helios readers allows for the construction of a "tailor-made" device that fits the user's needs regarding both the stimulation and detection module. OSL Helios readers are continually being developed to introduce further improvements and capabilities, such as battery power or heating options, to make the devices even more useful for dating and dosimetry research.

Acknowledgements

The authors would like to express their sincere gratitude to Professor David Sanderson for his valuable consultations regarding properly setting measurement parameters of the SUERC reader.

Supplementary material

Supplementary material containing additional **Figures S1–S4** and **Table S1** is available online at https://doi.org/10.20858/geochr/208873.

Data availability

All data was made open access on Zenodo and is digitally identified by DOI 10.5281/zenodo.15095948

Funding: MB was financed by project #101107989 - Lyoluminescence - HORIZON-MSCA-2022-PF-01. SK was financed through the DFG Heisenberg programme (#505822867). The research was partially carried out with the support of the Polish National Science Centre, contract number 2021/41/N/ST10/00169. This work was partly supported (RM and AM) by research project no. 2018/31/B/ST10/03966 from the Polish National Science Centre.

References

Alghamdi HMS, Sanderson DCW, Cresswell AJ and Fitzgerald S, 2024. Radiological or nuclear emergency OSL dosimetry using common-place salt. *Radiation Measurements* 174: 107141, DOI 10.1016/j.radmeas.2024.107141.

Alghamdi H, Sanderson D, Carmichael L, Cresswell A and Martin L, 2022. The use of portable OSL and IRSL measurements of NaCl in low dose assessments following a radiological or nuclear emergency. *Front. Public Health* 10: 969829, DOI 10.3389/fpubh.2022.969829.

Baril MR and Huntley DJ, 2003. Optical excitation spectra of trapped electrons in irradiated feldspars. *Journal of Physics: Condensed Matter* 15: 8011–8027, DOI 10.1088/0953-8984/15/46/017.

Ben-Melech N, Zeevi-Berger O, Porat N, Roskin J, Langgut D, Walker B and Gadot Y, 2024. Agricultural Terracing and Land Tenure in Late Medieval Southern Levant: The Case of Nahal Ein Karim, Jerusalem. *Environmental Archaeology:* 1–15, DOI 10.1080/14614103.2024.2371052.

Bernhardsson C, Christiansson M, Mattsson S and Rääf CL, 2009. Household salt as a retrospective dosemeter using optically stimulated luminescence. *Radiation and environmental biophysics* 48: 21–28, DOI 10.1007/s00411-008-0191-y.

Bøtter-Jensen L, Duller GAT, Murray AS and Banerjee D, 1999. Blue light emitting diodes for optical stimulation of quartz in retrospective dosimetry and dating. *Radiation Protection Dosimetry* 84(1–4): 335–340, DOI 10.1093/oxfordjournals.rpd.a032750.

Brill D, Jankaew K and Brückner H, 2016. Towards increasing the spatial resolution of luminescence chronologies - Portable luminescence reader measurements and standardized growth curves applied to a beach-ridge plain (Phra Thong, Thailand). *Quaternary Geochronology* 36: 134–147, DOI 10.1016/j.quageo.2016.09.003.

Bulur E, Èoksu HYG and Wahl W, 1998. Infrared (IR) stimulated luminescence from αlpha-Al2O3:C. *Radiaion Measurements* 29: 625–638, DOI 10.1016/S1350-4487(98)00076-6.

Buylaert JP, Thiel C, Murray AS, Vandenberghe DA, Yi S and Lu H, 2011. IRSL and post-IR IRSL residual doses recorded in modern dust samples from the Chinese Loess Plateau. *Geochronometria* 38: 432–440, DOI 10.2478/s13386-011-0047-0.

Carter J, Cresswell AJ, Kinnaird TC, Carmichael LA, Murphy S and Sanderson DCW, 2018. Non-Poisson variations in photomultipliers and implications for luminescence dating. *Radiation Measurements* 120: 267–273, DOI 10.1016/j.radmeas.2018.05.010.

Chruścińska A and Przegiętka K, 2005. Quartz TL decay due to optical bleaching. *Geochronometria* 24: 1–6.

Denis G, Rodriguez MG, Akselrod MS, Underwood TH and Yukihara EG, 2011. Time-resolved measurements of optically stimulated luminescence of Al2O3: C and Al2O3: C, Mg. *Radiation measurements* 46(12): 1457–1461, DOI 10.1016/j.radmeas.2011.06.054.

Euzen C, Chabaux F, Rixhon G, Preusser F, Eyrolle F, Chardon V, Zender AM, Badariotti D and Schmitt L, 2024. Multi-method geochronological approach to reconstruct post-1800 floodplain sedimentation in the Upper Rhine Plain, France. *Quaternary Geochronology* 83: 101561, DOI 10.1016/j.quageo.2024.101561.

Gray HJ, Mahan SA, Springer KB and Pigati JS, 2018. Examining the relationship between portable luminescence reader measurements and depositional ages of paleowetland sediments, Las Vegas Valley, Nevada. *Quaternary Geochronology* 48: 80–90, DOI 10.1016/j.quageo.2018.07.006.

Gray HJ, Jain M, Sawakuchi AO, Mahan SA and Tucker GE, 2019. Luminescence as a Sediment Tracer and Provenance Tool. *Reviews of Geophysics* 57: 987–1017, DOI 10.1029/2019RG000646.

Gray H, DuRoss C, Nicovich S and Gold R, 2022. Luminescence sediment tracing reveals the complex dynamics of colluvial wedge formation. *Science Advances* 8: eabo0747, DOI 10.1126/sciadv.abo0747.

Guérin G, Combès B, Lahaye C, Thomsen KJ, Tribolo C, Urbanova P, Guibert P, Mercier N and Valladas H, 2015. Testing the accuracy of a Bayesian central-dose model for single-grain OSL, using known-age samples. *Radiation Measurements* 81: 62–70. DOI 10.1016/j.radmeas.2015.04.002.

Hunter PG, Spooner NA, Smith BW and Creighton DF, 2012. Investigation of emission spectra, dose response and stability of luminescence from NaCl. *Radiation measurements* 47(9): 820–824, DOI 10.1016/j.radmeas.2012.01.005.

Huntley DJ, Godfrey-Smith DI and Thewalt MLW, 1985. Optical dating of sediments. *Nature* 313: 105–107, DOI 10.1038/313105a0.

Huntley DJ, Godfrey-Smith DI and Haskell EH, 1991. Light-induced emission spectra from some quartz and feldspars. *International Journal of Radiation Applications and Instrumentation*. *Part D. Nuclear Tracks and Radiation Measurements* 18: 127–131, DOI 10.1016/1359-0189(91)90104-P.

Ikeya M and Furusawa M, 1989. A portable spectrometer for ESR microscopy, dosimetry and dating. *International Journal of Radiation Applications and Instrumentation. Part A. Applied Radiation and Isotopes* 40(10–12): 845–850, DOI 10.1016/0883-2889(89)90005-1.

Ikeya M, Katakuse I and Ichihara T, 1990. Portable thermoluminescence reader for dosimetry and dating in fields. *Journal of Nuclear Science and Technology* 27(2): 188–190, DOI 10.3327/jnst.27.188.

Karampiperi M, Rääf CL and Bernhardsson C, 2024. Evaluation of a portable OSL/IRSL reader for radiation dose assessment of NaCl pellets–in situ individualised screening during R/N emergencies. *Radiation Measurements* 179: 107323, DOI 10.1016/j.radmeas.2024.107323.

Kim H, Park CY, Kim SI, Kim MC and Lee J, 2024. Development of a prototype TL/OSL reader for on-site use in a large-scale radiological accident. *Nuclear Engineering and Technology* 56(6): 2113–2119, DOI 10.1016/j.net.2024.01.019.

Kinnaird TC, Sanderson DC and Bigelow GF, 2015. Feldspar SARA IRSL dating of very low dose rate aeolian sediments from Sandwick South, Unst, Shetland. *Quaternary Geochronology* 30: 168–174. DOI 10.1016/j.quageo.2015.02.019.

Kook MH, Murray AS, Lapp T, Denby PH, Ankjærgaard C, Thomsen K, Jain M, Choi Kim JH and Kim GH, 2011. A portable luminescence dating instrument. *Nuclear Instruments and Methods in Physics Research Section B: Beam Interactions with Materials and Atoms* 269(12): 1370–1378, DOI 10.1016/j.nimb.2011.03.014.

Kreutzer S, Martin L, Guérin G, Tribolo C, Selva P and Mercier N, 2018. Environmental dose rate determination using a passive dosimeter: techniques and workflow for α-Al2O3: C chips. *Geochronometria* 45(1): 56–67, DOI 10.1515/geochr-2015-0086.

Kreutzer S and Burow C, 2022. xlum: read, write, and convert XLUM Data (v0.1.0). Zenodo, DOI 10.5281/zenodo.7362364.

Kreutzer S, Grehl S, Höhne M, Simmank O, Dornich K, Adamiec G, Burow C, Roberts HM and Duller GA, 2023. XLUM: an open data format for exchange and long-term preservation of luminescence data. *Geochronology* 5(1): 271–284, DOI 10.5194/gchron-5-271-2023.

Kreutzer S, Burow C, Dietze M, Fuchs MC, Schmidt C, Fischer M, Friedrich J, Mercier N, Philippe A, Riedesel S, Autzen M, Mittelstrass D, Gray HJ, Galharret JM and Colombo M, 2024. *Luminescence: Comprehensive luminescence dating data analysis*. version: 0.9.26, URL https://CRAN.R-project.org/package=Luminescence; DOI 10.32614/CRAN.package.Luminescence.

Lomax J, Mittelstraß D, Kreutzer S and Fuchs M, 2015. OSL, TL and IRSL emission spectra of sedimentary quartz and feldspar samples. *Radiation Measurements* 81: 251–256, DOI 10.1016/j.radmeas.2009.04.001.

Mandowski A, Mandowska E, Kokot L, Bilski P, Olko P and Marczewska B, 2010. Portable system for identifying radiation hazards using OSL microdetectors (in Polish). *Elektronika: konstrukcje, technologie, zastosowania* 51(2): 136–138.

Marczewska B, Bilski P, Wróbel D and Kłosowski M, 2016. Investigations of OSL properties of LiMgPO4: Tb, B based dosimeters. *Radiation Measurements* 90: 265–268, DOI 10.1016/j.radmeas.2016.02.004.

Marczewska B, Sas-Bieniarz A, Bilski P, Gieszczyk W, Kłosowski M and Sądel M, 2019. OSL and RL of LiMgPO4 crystals doped with rare earth elements. *Radiation Measurements* 129: 106205, DOI 10.1016/j.radmeas.2019.106205.

Moska P, Bluszcz A, Poręba G, Tudyka K, Adamiec G, Szymak A and Przybyła A, 2021. Luminescence dating procedures at the Gliwice Luminescence Dating Laboratory *Geochronometria* 48: 1–15, DOI 10.2478/geochr-2021-0001.

Mrozik A, Kulig D, Marczewska B and Bilski P, 2017. Dose estimation based on OSL signal from banknotes in accident dosimetry. *Radiation Measurements* 101: 1–6, DOI 10.1016/j.radmeas.2017.04.012.

Mrozik A and Bilski P, 2021. Popular medicines as radiation sensors. *IEEE Sensors Journal* 21(15): 16637–16643, DOI 10.1109/JSEN.2021.3082285.

Munyikwa K, Kinnaird TC and Sanderson DC, 2021. The potential of portable luminescence readers in geomorphological investigations: a review. *Earth Surface Processes and Landforms* 46(1): 131–150, DOI 10.1002/esp.4975.

Murray AS and Wintle AG, 2000. Luminescence dating of quartz using an improved single-aliquot regenerative-dose protocol. *Radiation Measurements* 32: 57–73, DOI 10.1016/s1350-4487(99)00253-x.

Muñoz-Salinas E, Bishop P, Sanderson DC and Zamorano J, 2011. Interpreting luminescence data from a portable OSL reader: three case studies in fluvial settings. *Earth Surface Processes and Landforms* 36: 651–660, DOI 10.1002/esp.2084.

Nitundil S, Stone A and Srivastava A, 2023. Applicability of using portable luminescence reader for rapid age-assessments of dune accumulation in the Thar desert, India. *Quaternary Geochronology* 78: 101468, DOI 10.1016/j.quageo.2023.101468.

Perks CA, Yahnke C and Million M, 2008. Medical dosimetry using Optically Stimulated Luminescence dots and microStar readers. *In Proceedings of 12th International congress of the International Radiation Protection Association*, Buenos Aires, Argentina. https://inis.iaea.org/records/m0bpp-xjw53.

Poolton NRJ, Bøtter-Jensen L, Wintle AG, Jakobsen J, Jørgensen F and Knudsen KL, 1994. A portable system for the measurement of sediment OSL in the field. *Radiation Measurements* 23(2–3): 529–532. DOI 10.1016/1350-4487(94)90093-0.

Porat N, López GI, Lensky N, Elinson R, Avni Y, Elgart-Sharon Y, Faershtein G and Gadot Y, 2019. Using portable OSL reader to obtain a time scale for soil accumulation and erosion in archaeological terraces, the Judean Highlands, Israel. *Quaternary Geochronology* 49: 65–70, DOI 10.1016/j.quageo.2018.04.001.

Rawat NS, Dhabekar B, Kulkarni MS, Muthe KP, Mishra DR, Soni A, Gupta SK and Babu DAR, 2014. Optimization of CW-OSL parameters for improved dose detection threshold in Al2O3:C. *Radiation Measurements* 71: 212–216, DOI 10.1016/j.radmeas.2014.02.013.

R Core Team, 2025. R: A language and environment for statistical computing. version: v4.3.2, URL https://r-project.org/, (accessed 2025-02-10).

Richter D, Richter A and Dornich K, 2015. Lexsyg smart—a luminescence detection system for dosimetry, material research and dating application. *Geochronometria* 42(1): 202–209, DOI 10.1515/geochr-2015-0022.

Richter D, Słonecka I, Schischke S and Dornich K, 2018. myOSL–A new series of portable and stationary equipment for OSL-dosimetry based ON BeO. In RAD Conference Proceedings Vol. 3, pp. 132–137, DOI 10.21175/RadProc.2018.29.

Rizza M, Rixhon G, Valla PG, Gairoard S, Delanghe D, Fleury J, Tal M and Groleau S, 2024. Revisiting a proof of concept in quartz-OSL bleaching processes using sands from a modern-day river (the Séveraisse, French Alps). *Quaternary Geochronology* 82: 101520, DOI 10.1016/j.quageo.2024.101520.

Rodriguez-Lazcano Y, Correcher V and Garcia-Guinea J, 2012. Luminescence emission of natural NaCl. *Radiation Physics and Chemistry* 81(2): 126–130. DOI 10.1016/j.radphyschem.2011.07.012.

Sanderson DC and Murphy S, 2010. Using simple portable OSL measurements and laboratory characterisation to help understand complex and heterogeneous sediment sequences for luminescence dating. *Quaternary Geochronology* 5(2–3): 299–305, DOI 10.1016/j.quageo.2009.02.001.

Singarayer JS and Bailey RM, 2003. Further investigations of the quartz optically stimulated luminescence components using linear modulation. *Radiation Measurements* 37: 451–458, DOI 10.1016/S1350-4487(03)00062-3.

Spooner NA, Smith BW., Williams OM, Creighton DF, McCulloch I, Hunter PG, Questiaux DG and Prescott JR, 2011. Analysis of luminescence from common salt (NaCl) for application to retrospective dosimetry. *Radiation Measurements* 46(12): 1856–1861, DOI 10.1016/j.radmeas.2011.06.069.

Srivastava A, Kinnaird T, Sevara C, Holcomb JA and Turner S, 2023. Dating Agricultural Terraces in the Mediterranean Using Luminescence: Recent Progress and Challenges. *Land* 12: 716, DOI 10.3390/land12030716.

Stone A, Bateman MD, Burrough SL, Garzanti E, Limonta M, Radeff G and Telfer MW, 2019. Using a portable luminescence reader for rapid age assessment of aeolian sediments for reconstructing dunefield landscape evolution in southern Africa. *Quaternary Geochronology* 49: 57–64, DOI 10.1016/j.quageo.2018.03.002.

Stone A, Bateman MD, Sanderson D, Burrough SL, Cutts R and Cresswell A, 2024. Probing sediment burial age, provenance and geomorphic processes in dryland dunes and lake shorelines using portable luminescence data. *Quaternary Geochronology* 82: 101542, DOI 10.1016/j.quageo.2024.101542.

Thomsen KJ, Murray AS and Bøtter-Jensen L, 2005. Sources of variability in OSL dose measurements using single grains of quartz. *Radiation measurements* 39(1): 47–61, DOI 10.1016/j.radmeas.2004.01.039.

Thomsen KJ, Jain M, Murray AS, Denby PM, Roy N and Bøtter-Jensen L, 2008. Minimizing feldspar OSL contamination in quartz UV-OSL using pulsed blue stimulation. *Radiation Measurements* 43(2–6): 752–757, DOI 10.1016/j.radmeas.2008.01.020.

Turner S, Kinnaird T, Varinlioğlu G, Şerifoğlu TE, Koparal E, Demirciler V, Athanasoulis D, Ødegård K, Crow J, Jackson M, Bolòs J, Sánchez-Pardo JC, Carrer F, Sanderson D and Turner A, 2021. Agricultural terraces in the Mediterranean: medieval intensification revealed by OSL profiling and dating. *Antiquity* 95: 773–790, DOI 10.15184/aqy.2020.187.

Umisedo NK, Yoshimura EM, Gasparian PB, Yukihara EG, 2010. Comparison between blue and green stimulated luminescence of Al2O3:C. *Radiation Measurements* 45(2): 151–156. DOI 10.1016/j.radmeas.2010.02.001.

Winnicki J, 1997. Geological structure of the Trzebnica Hills in the light of new investigation. *Geological Quarterly* 41(3): 365–380.

Yukihara EG and McKeever SWS, 2006. Spectroscopy and optically stimulated luminescence of Al2O3: C using time-resolved measurements. *Journal of Applied Physics* 100(8): 083512, DOI 10.1063/1.2357344.

Yukihara EG, 2011. Luminescence properties of BeO optically stimulated luminescence (OSL) detectors. *Radiation Measurements* 46(6–7): 580–587, DOI 10.1016/j.radmeas.2011.04.013.

Yukihara EG, Andrade AB and Eller S, 2016. BeO optically stimulated luminescence dosimetry using automated research readers. *Radiation Measurements* 94: 27–34, DOI 10.1016/j.radmeas.2016.08.008.

Yukihara EG, McKeever SWS, Andersen CE, Bos AJJ, Bailiff IK, Yoshimura EM, Sawakuchi GO, Bossin L and Christensen JB, 2022. Luminescence dosimetry. *Nature Reviews Methods Primers* 2: 26, DOI 10.1038/s43586-022-00102-0.

Zero-Rad, Poland, 2025. Last access: 2025-01-23, URL https://zero-rad.com/